



Tunable THz perfect absorber with two absorption peaks based on graphene microribbons

Gu, Mingyue; Xiao, Binggang; Xiao, Sanshui

Published in:
Micro & Nano Letters

Link to article, DOI:
[10.1049/mnl.2017.0742](https://doi.org/10.1049/mnl.2017.0742)

Publication date:
2018

Document Version
Peer reviewed version

[Link back to DTU Orbit](#)

Citation (APA):
Gu, M., Xiao, B., & Xiao, S. (2018). Tunable THz perfect absorber with two absorption peaks based on graphene microribbons. *Micro & Nano Letters*, 13(5), 631-635. <https://doi.org/10.1049/mnl.2017.0742>

General rights

Copyright and moral rights for the publications made accessible in the public portal are retained by the authors and/or other copyright owners and it is a condition of accessing publications that users recognise and abide by the legal requirements associated with these rights.

- Users may download and print one copy of any publication from the public portal for the purpose of private study or research.
- You may not further distribute the material or use it for any profit-making activity or commercial gain
- You may freely distribute the URL identifying the publication in the public portal

If you believe that this document breaches copyright please contact us providing details, and we will remove access to the work immediately and investigate your claim.

A tunable terahertz perfect absorber with two absorption peaks based on graphene micro-ribbons

Mingyue Gu¹, Binggang Xiao^{1,2} and Sanshui Xiao²

¹ College of Information Engineering, China Ji Liang University, Hangzhou 310018, People's Republic of China

² Department of Photonics Engineering, Technical University of Denmark, Lyngby DK-2800, Denmark

E-mail: bgxiao@cjl.u.edu.cn

Perfect absorption is characterized by the complete suppression of incident and reflected electromagnetic wave, and complete dissipation of the incident energy. In this paper, a tunable perfect terahertz (THz) absorber with two absorption peaks based on graphene is presented. The proposed structure consists of graphene micro-ribbons sandwiched between aluminum oxide (Al₂O₃) strips and polymethyl methacrylate (PMMA) slab on a silicon dioxide (SiO₂) layer which is covered by periodic gold ribbons, and the SiO₂ layer is supported by gold substrate. The influence of the structural parameters on the absorption performance was analyzed too. Specially, graphene can be used to design tunable terahertz devices due to its tunability of sheet conductivity which could be controlled by applying a bias voltage or chemical doping. A single-band perfect absorption can be achieved when the chemical potential is set to 0.1eV. Interestingly, when the chemical potential changed to 0.6eV, a dual-band absorption spectrum is obtained with absorption efficiency of the two peaks more than 90%. These results imply that the characteristics of graphene based surface plasmon could be used to design novel THz devices in future.

1. Introduction: In the past few years, the THz technology has attracted great attention to the researchers [1, 2]. But compared to microwave band, the study of THz detectors and absorbers are still insufficient [3]. The main reason is the lack of natural material that can response to strong terahertz waves and difficult to fabricate device [4]. Nowadays, the THz detection devices include Quantum well detector and metamaterial absorbers, these absorbers can be used in the design of the detector or imager, and generally composed of an electric split-ring resonator layer [5], or patch layer [6]. However, most of the metamaterial absorbers are metal-based which operate only at some fixed frequency, limiting practical application [7, 8].

Graphene as a two-dimensional carbon material has emerged as promising material for optoelectronics due to its excellent electric properties such as optical transparency, high electronic mobility, and controlled conductivity [9-12]. These extraordinary electronic properties make graphene a promising candidate for low loss electronic devices. At THz frequencies, graphene with appropriate doping can generate surface plasmon polaritons which have greater confinement of the electromagnetic energy, lower propagation loss, and could lead to strong light-graphene interactions [13, 14]. Graphene-based THz absorbers are usually made up of patterned graphene organized in a periodic super lattice structures which could excite SPPs resonance when the electromagnetic wave impinges on graphene, and leading to plasmonic absorption enhancement. Due to the carrier concentration and the conductivity of graphene can be controlled by chemical doping and bias voltage, so the performance of graphene-based absorber is more flexible than that of metal-based absorber. Up to now, a lot of different devices based patterned graphene have been proposed and studied in the THz or infrared region, such as perfect absorbers based on micro or nanoribbons, optical polarization converters based on asymmetric graphene nanocrosses, and so on [15-22]. Recently, many efforts have been made to achieve dual-band terahertz absorbers. In 2015, Su et al. proposed a THz dual-band metamaterial absorber based on ten graphene/MgF₂ bilayers stacking structure [23], and in 2016, Chen et al. demonstrated dual-frequency absorption by stacking double layer graphene metasurfaces composed of a graphene outer ring nesting a cross-shaped resonator with various geometric dimensions [24]. However, these structures mentioned above rely on multilayer patterned graphene which leads to the challenges in fabrication. Here, we present a tunable THz absorber with two absorption peaks based on

graphene micro ribbons. The structure proposed here requires only one layer of graphene to achieve dual-band absorption, which of course simplifies the fabrication process. Due to the conductivity of graphene can be tuned on purpose, the dual-band THz absorber is achieved here. We make use of the advantages of nanostructure of a metal-insulator-metal (MIM) perfect light absorber, which could realize perfect absorption due to effects of a plasmon guide mode with an extra small dielectric gap [25]. So, the structure of metal-insulator-graphene-insulator-metal (MIGIM) is proposed. The performances of proposed structure have been verified with numerical simulation.

2. Structure and calculation method: The proposed periodic MIGIM structure is plotted in Fig. 1a. And the two-dimensional cross section diagram of the unit cell is shown in Fig. 1b. From top to bottom, they are a gold micro strip, a micro ribbon graphene sheet sandwiched between the Al₂O₃ strip and PMMA slab, the SiO₂ dielectric substrate and the gold ground plane, respectively, tightly stacked to form the unit cell. The geometrical parameters of the unit cell are set after performance optimization by numerical simulation. The width w of the ribbon is initially set to 7 μ m. The separations between neighbouring strips is fixed at 10.75 μ m. The thickness h of Al₂O₃, the graphene sheet Δ , the PMMA layer and SiO₂ substrate are set to 210nm, 1nm, 85nm, and 3 μ m respectively. The thickness of gold micro ribbon and the ground plane are 0.5 μ m. Due to the thickness of the gold layer used here is much larger than the typical skin depth in the THz regime, so the reflection is the only factor limiting the absorption. Here the conductivity of gold is 4.7*10⁷ S/m, and the relative permittivity of Al₂O₃ strips $\epsilon_{Al_2O_3}$, PMMA film ϵ_{PMMA} , and silicon dioxide ϵ_{SiO_2} are set as 3, 2.3, and 4 respectively. The Al₂O₃ and PMMA layers are used as isolating spacers to keep higher carrier mobility of the graphene micro-ribbons than only utilizing SiO₂ layers. At the end of z direction, the graphene micro-ribbons are connected to each other, therefore all the graphene micro-ribbons can keep the same chemical potential [15].

The graphene was numerically modeled by a thin layer (with thickness $\Delta=1$ nm) of relative permittivity $\epsilon_{GR}=1+i\sigma_{GR}/\omega\Delta\epsilon_0$, the σ_{GR} as the surface conductivity of graphene sheet which can be derived using the well-known Kubo formula is described with interband and intraband contributions as [26]

$$\sigma_{GR} = \frac{ie^2}{4\pi\hbar} \ln\left(\frac{2|\mu_c| - (\omega + i2\Gamma)\hbar}{2|\mu_c| + (\omega + i2\Gamma)\hbar}\right) + \frac{ie^2 k_B T}{\pi\hbar^2 (\omega + i2\Gamma)} \left(\frac{\mu_c}{k_B T} + 2 \ln e^{\frac{-\mu_c}{k_B T}} + 1 \right) \quad (1)$$

Where e , \hbar and K_B are universal constants representing the electron charge, reduced Planck's and Boltzmann's constant, respectively. T is the temperature and is fixed to 300K. μ_c and 2Γ ($2\Gamma = \hbar/\tau$, τ is the electron-phonon relaxation time) are physical parameters of the graphene sheet accounting for the chemical potential (i.e. Fermi energy E_f) and the intrinsic losses, respectively. We assumed $\Gamma = 0.1\text{meV}$, which is based on theoretical estimation of maximum mobility in graphene [27].

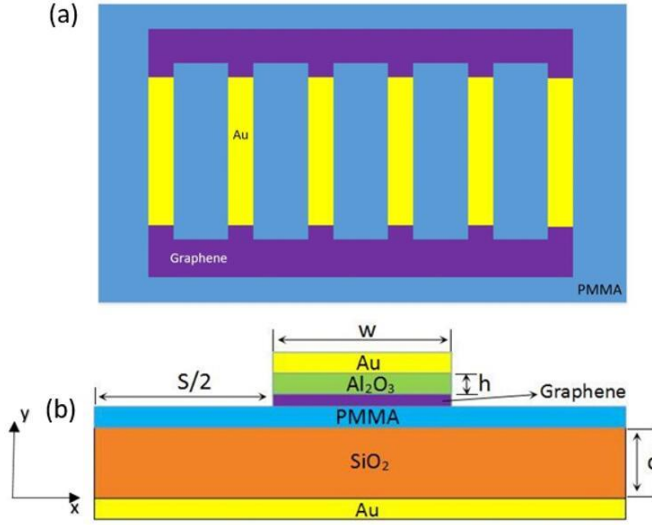


Fig. 1 Structure diagram of the proposed structure. Top-view illustration of the proposed graphene micro-ribbon array (Fig. 1a) and cross section of the one unit of the proposed structure (Fig. 1b)

With equations of graphene relative permittivity $\epsilon_{GR} = 1 + i\sigma_{GR}/\omega\epsilon_0$, we can calculate the relationship between relative permittivity of graphene and frequency at different chemical potential, as shown in Fig. 2. When the chemical potential of graphene from 0.1eV increased to 0.7eV, the absolute value of real part and imaginary part of the relative permittivity become larger too. Interestingly, one sees from Fig. 2a that in the THz range the real part of relative permittivity for graphene is negative, thus in the THz region, a graphene sheet does have the property of a metal, which can support a transverse magnetic electromagnetic SPP surface wave. But graphene has a lower loss compared with other noble metal. Therefore, graphene becomes a promising candidate to take place of noble metal in the THz regime.

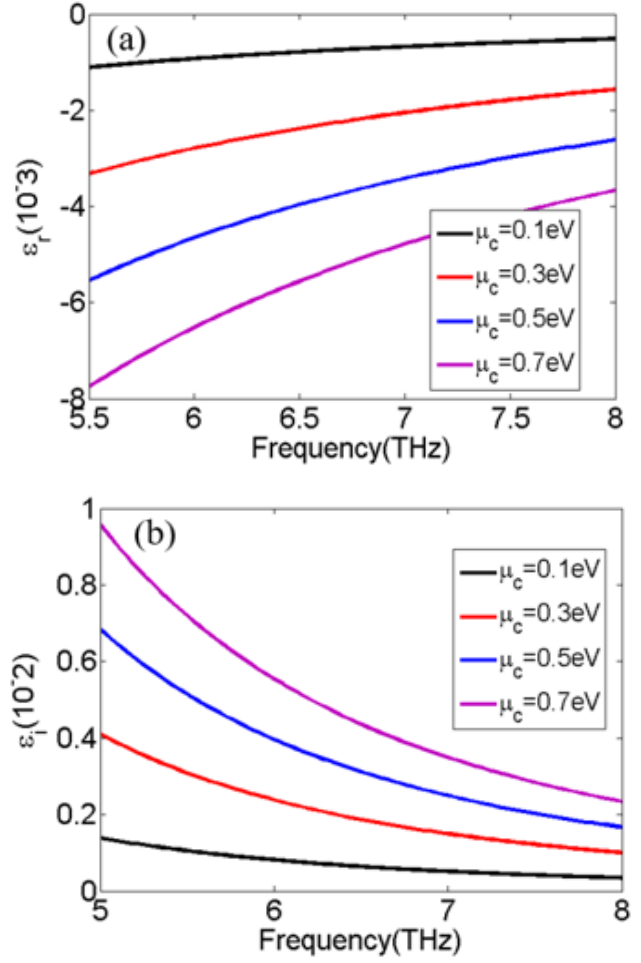


Fig. 2 Real (Fig. 2a) and imaginary (Fig. 2b) parts of relative permittivity of 1nm thickness sheet as function of frequency as well as chemical potential

3. Simulations and results: In this paper, we assume a plane wave normally incident on the structures. Since the whole absorber is a periodic structure, so we only need to analyze one unit cell using the periodic boundary condition according to floquet theorem. And the calculation is performed by using a commercial available finite element method software package (COMSOL). We rely on two-dimensional (2D) full-wave simulation to analyze the absorptivity performance, and the direct solver of frequency domain analysis is used to evaluate the absorption. Due to the Au at the bottom of the structure can be seen as PEC in THz range, so the transmission can be ignored in the entire frequency range investigated. The absorption can use the formula of $A(\omega) = 1 - R(\omega) - T(\omega)$, reflection $R(\omega)$ and transmission $T(\omega)$ are obtained from the frequency-dependent S-parameter $S_{11}(\omega)$ and $S_{21}(\omega)$, $R(\omega) = |S_{11}(\omega)|^2$ and $T(\omega) = |S_{21}(\omega)|^2$. Due to the thickness of the gold substrate used here is much larger than the typical skin depth in the THz regime, so the transmission is almost zero in the entire frequency range investigated.

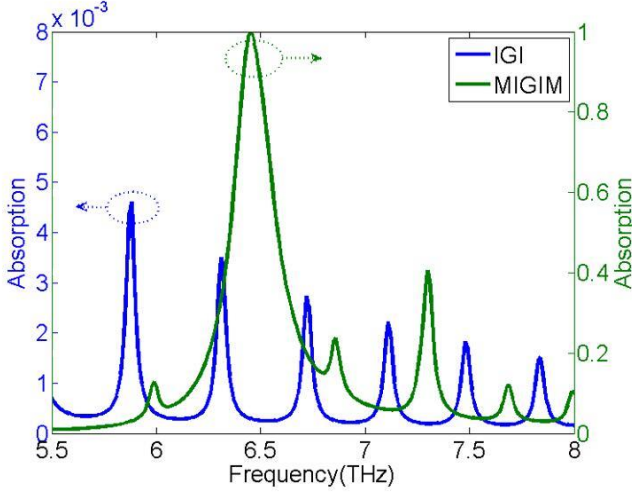


Fig. 3 The absorption spectra of MIGIM and IGI microstructure.

In order to reveal the physical insight, we discuss the absorbance of MIGIM and IGI (without top and bottom gold) microstructure under TM polarized incident electromagnetic wave, as shown in Fig. 3. It shows that the IGI microstructure has several absorption peaks with weakly absorbance. These resonance of the periodic array are associated with leaky plasmonic modes [28]. However, for MIGIM structure, the absorbance of graphene has been significantly enhanced up to 99% at $f=6.45\text{THz}$, which is much more than the IGI microstructure. So we focus on the absorption properties with MIGIM structure in the following discussion.

Then we consider effects of changing the height h of Al_2O_3 strips as shown in Fig. 4a. Similar to the MIM plasmonic structure, the resonance characteristics of proposed structure are very sensitive to the thickness of Al_2O_3 strips. When the height h increases from 160nm to 360nm, the phenomenon of blue shift in the absorption peak frequency is obvious due to the expansion of the plasmonic gap. With the increases of h , the plasmon coupling of near fields between graphene and gold ribbon become stronger until a maximum absorption efficiency is realized at $h=210\text{nm}$, and then becomes weaker. Besides, with the increases of the spacer, the absorption bandwidth broadens to 0.1THz and the efficiency is above 90% when the thickness ranges from 260nm to 310nm. These effects can be used to design broadband absorbers in the THz regime.

Next we investigate the influence of the thickness of silicon dioxide on the absorption of graphene, as demonstrated in Fig. 4b. When d increases from $2.6\mu\text{m}$ to $3.2\mu\text{m}$, it obviously shows that resonance enhancement and attenuation around 6.45THz , and there is an optimal height of silicon dioxide layer, at which the absorption peak frequency nearly 99.9%. It means that with the increases of d , the plasmon coupling strength gets stronger until a perfect absorption is achieved and then becomes weaker, which is due to the coupling of plasmon between each graphene strip and continuous metal substrate.

And then, we discuss the influence of different width of metal on the absorption of graphene ribbons, as shown in Fig. 4c. As w increases from $6.8\mu\text{m}$ to $7.2\mu\text{m}$, the absorption peak frequency of graphene is red shifted, because the micro ribbon acts as a Fabry-Perot resonator for the horizontal plasmon guided mode and the width of micro ribbon have a great impact on the resonance frequency. So, with the increment of the micro ribbon width, the effective resonance wavelength of localized surface plasmon increased too. And the most important thing is that the absorption efficiency is nearly 99.9% at different width of micro ribbons, therefore we could easily get different absorption peak frequency by select proper width of micro

ribbons. Through the above analysis, we know that the different absorption spectrum can be obtained by changing the width of strip.

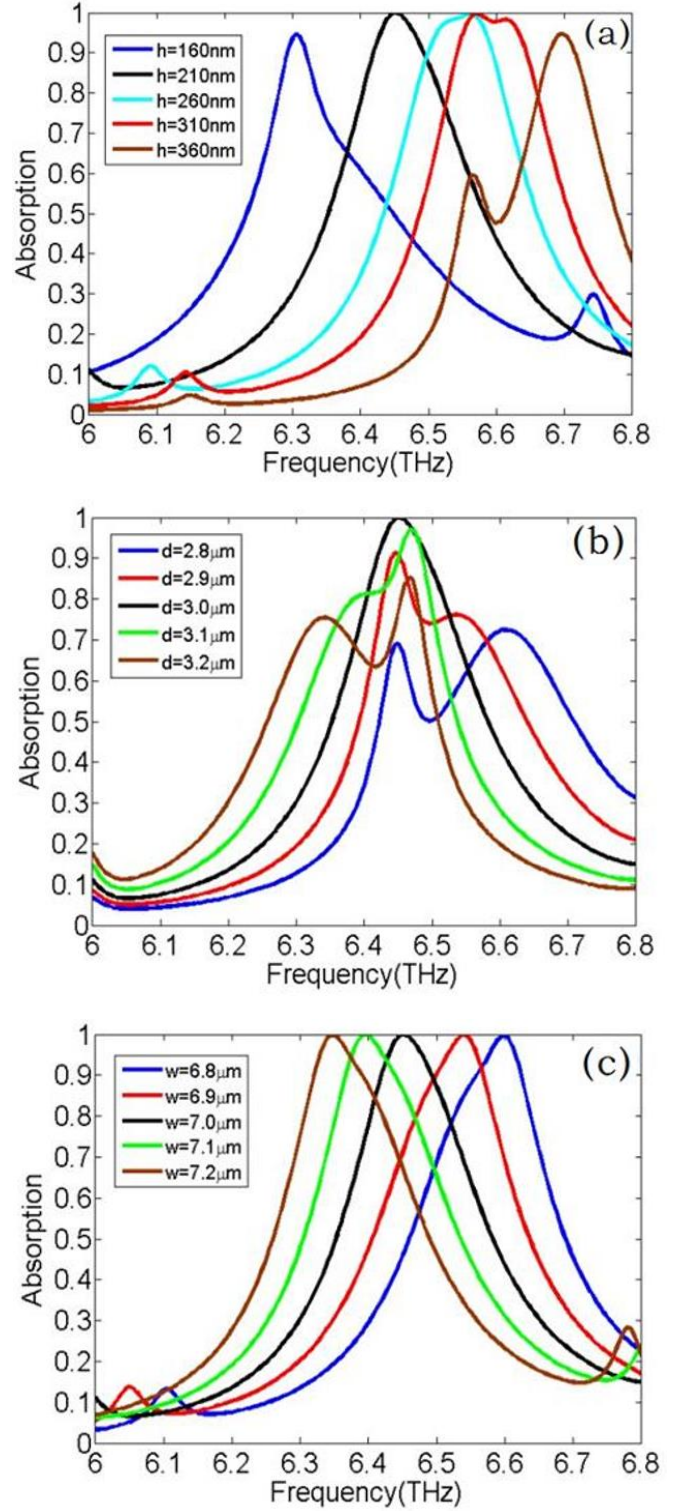


Fig. 4 The absorption spectra for different h , where $d=3\mu\text{m}$, $w=7\mu\text{m}$, $\mu_c=0.1eV$ (Fig.4a). The absorption spectra for different d , where $h=210\text{nm}$, $w=7\mu\text{m}$, $\mu_c=0.1eV$ (Fig. 4b). The absorption spectra for different w , where $h=210\text{nm}$, $d=3\mu\text{m}$, $\mu_c=0.1eV$ (Fig. 4c).

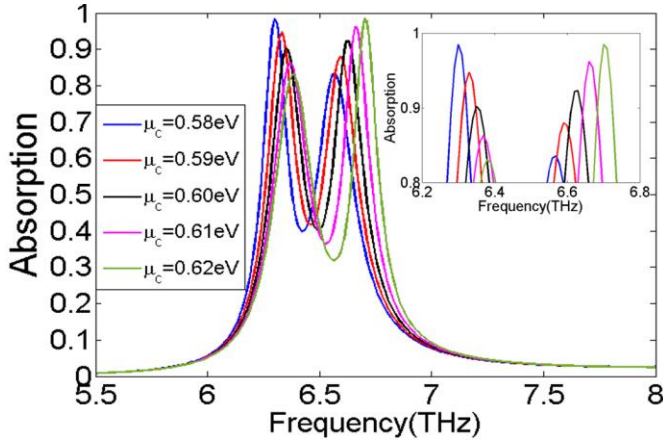


Fig. 5 The absorption spectra for different μ_c , where $h=210\text{nm}$, $d=3\mu\text{m}$, $w=7\mu\text{m}$, the inset shows the absorption over 80%.

However, for graphene, one of the most important properties is conductivity which can be adjusted by applying a bias voltage. The absorption spectra under different chemical potential of graphene micro-ribbon is depicted in Fig. 5. The frequency of the absorption resonance experiences the blue shift with the increase of chemical potential. It should be mentioned that two absorption peaks can be achieved in the tuning range. Therefore, by applying a gate voltage on the graphene layer, the chemical potential and thus the conductivity of graphene can be controlled on purpose [29].

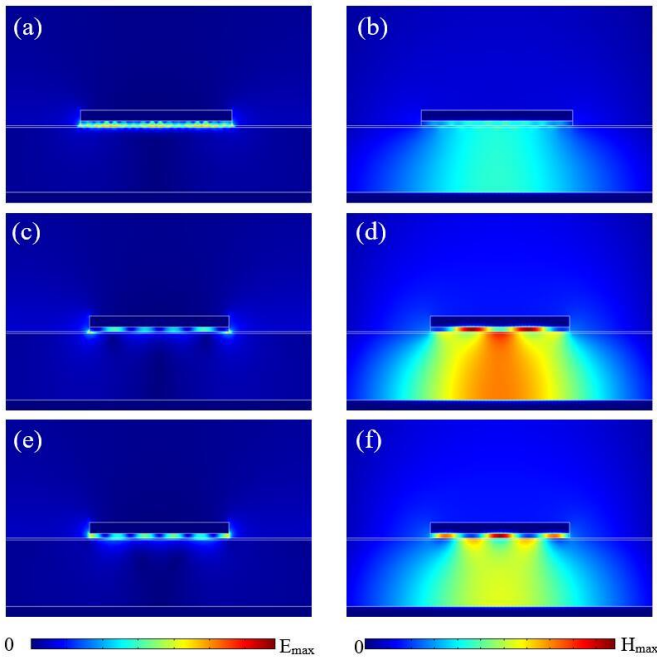


Fig. 6 Electric field and magnetic field distribution at different absorption peak frequency, where $w=7\mu\text{m}$. Electric field (Fig. 6a) and magnetic field (Fig. 6b) at $f=6.45\text{THz}$, $\mu_c=0.1\text{eV}$. Electric field (Fig. 6c) and magnetic field (Fig. 6d) at $f=6.35\text{THz}$, $\mu_c=0.6\text{eV}$. Electric field (Fig. 6e) and magnetic field (Fig. 6f) at $f=6.63\text{THz}$, $\mu_c=0.6\text{eV}$.

The obtained results can be further explained by the distributions of the electric field and magnetic field as shown in Fig. 6. The presented electric field distributions in Fig. 6a, 6c and 6e shows the electric field are strongly trapped surrounding the graphene due to the occurrence of localized surface plasmons resonance in graphene ribbons, and enhanced the absorption of incident energy. Each peak on the absorption spectrum corresponds to a graphene surface plasmons

resonance in the micro-ribbon. These resonances correspond to the excitation of higher order graphene surface plasmons waveguide mode, which have been discussed in the Ref. 28. From Fig. 6b, 6d and 6f can know that the magnetic field is guided between each gold micro-ribbon and gold substrate. The field distribution shows that incident field confinement in the surround of graphene layers as the guided gap-plasmon mode and induce the effects of near field enhancement and THz energy concentration. The input fields penetrating graphene dissipate in the dielectric and contribute to the enhanced absorption inside graphene.

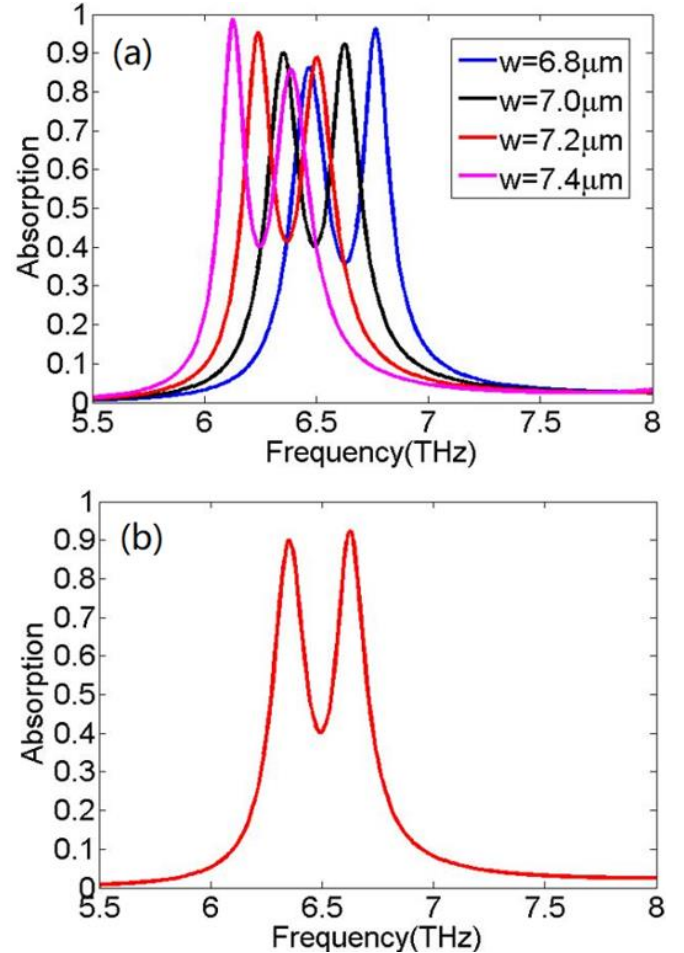


Fig. 7 The absorption spectrum of the proposed structure as a function of the width of micro-ribbon, where $\mu_c=0.6\text{eV}$ (Fig. 7a). The absorption spectrum of the proposed dual-band absorber, where $\mu_c=0.6\text{eV}$, $w=7\mu\text{m}$ (Fig. 7b).

In addition, the dual-band absorption spectrum for different widths of micro-ribbon has been calculated and displayed in Fig. 7a. It shows that with the increase of w , the two absorption peaks are red shifting due to the effective wavelength of localized surface plasmon increased. This is analogous to the above analysis of the single band absorption. When μ_c equals to 0.6eV and the width of micro-ribbon is fixed at $7\mu\text{m}$, the dual-band absorber can simultaneously work at two frequencies with its absorptivity being 90% for 6.35THz and 92% for 6.63THz as shown in Fig. 7b.

Compared with other dual-band metamaterial absorbers, what we propose here has the advantage with respect to the simplicity of design, while keeping high performance. The structure proposed here has the relatively large frequency ratio (f_u/f_l) and high absorption efficiency, where f_u and f_l are the central frequencies of the higher and lower

absorbing bands, respectively. For example, Su et al. proposed dual-band absorber whose frequency ratio is about 1.02 [23], slightly less than our 1.04. Our proposed design reaches maximum absorption efficiency with 99%, higher than 95% proposed by Taghvaei et al. [30].

4. Conclusion: In conclusion, a dual-band tunable THz absorber based on graphene plasmonics is proposed and discussed here. Simulation results show that the MIGIM absorber possess strong absorption of THz radiation. And a dual band excellent absorption spectrums can be achieved by adjusting the parameters of the structure. Particularly, the absorption peak frequency can be adjusted activity by tuning the bias voltage on the graphene layer instead of changing the geometric parameters, which improves the flexibility and controllability compared to metallic-based absorbers. Thus the proposed absorber may provide an opportunity to choose the desirable absorption frequency band through graphene micro-ribbons and could be used to design cloaking objects and other THz devices in future.

5. Acknowledgments: This work was supported by 2016 Zhejiang Provincial Natural Science Foundation [grant number LY16F010010]; in part by 2015 Zhejiang Province Public Welfare of International Cooperation Project [grant number 2015C34006].

6. References

- [1] Cao, W.; Song, C.; Lanier, T. E.; Singh, R.; O'Hara, J. F.; Dennis, W. M.; Zhao, Y.; Zhang, W.: 'Tailoring terahertz plasmons with silver nanorod arrays', *Scientific reports*, **2013**, 3, (5), p. 1766.
- [2] Purkayastha, A.; Srivastava, T.; Jha, R.: 'Ultrasensitive THz-Plasmonics gaseous sensor using doped graphene', *Sensors and Actuators B: Chemical*, **2016**, 227, pp. 291-295.
- [3] Mittleman, D. M.: 'Frontiers in terahertz sources and plasmonics', *Nature Photonics*, **2013**, 7, (9), pp. 666-669.
- [4] Ma, Y.; Chen, Q.; Grant, J.; Saha, S. C.; Khalid, A.; Cumming, D. R.: 'A terahertz polarization insensitive dual band metamaterial absorber', *Optics Letters*, **2011**, 36, (6), pp. 945-947.
- [5] Tao, H.; Landy, N. I.; Bingham, C. M.; Zhang, X.; Averitt, R. D.; Padilla, W. J.: 'A metamaterial absorber for the terahertz regime: Design, fabrication and characterization', *Optics express*, **2008**, 16, (10), pp. 7181-7188.
- [6] Cheng, Y.; Nie, Y.; Gong, R.: 'A polarization-insensitive and omnidirectional broadband terahertz metamaterial absorber based on coplanar multi-squares films', *Optics & Laser Technology*, **2013**, 48, pp. 415-421.
- [7] Tao, H.; Bingham, C.; Pilon, D.; Fan, K.; Strikwerda, A.; Shrekenhamer, D.; Padilla, W.; Zhang, X.; Averitt, R.: 'A dual band terahertz metamaterial absorber', *Journal of physics D: Applied physics*, **2010**, 43, (22), p. 225102.
- [8] Wen, Q.-Y.; Zhang, H.-W.; Xie, Y.-S.; Yang, Q.-H.; Liu, Y.-L.: 'Dual band terahertz metamaterial absorber: Design, fabrication, and characterization', *Applied Physics Letters*, **2009**, 95, (24), p. 241111.
- [9] Ding, Y.; Zhu, X.; Xiao, S.; Hu, H.; Frandsen, L. H.; Mortensen, N. A.; Yvind, K.: 'Effective electro-optical modulation with high extinction ratio by a graphene-silicon microring resonator', *Nano letters*, **2015**, 15, (7), pp. 4393-4400.
- [10] Goncalves, P.A.D.; Dias, E.J.C.; Xiao, S.; Vasilevskiy, M.I.; Mortensen, N.A.; Peres, N.M.R.: 'Graphene Plasmons in Triangular Wedges and Grooves', *ACS Photonics* **2016**, 3 (11), pp.2176-2183.
- [11] Wang, Z.; Li, T.; Almdal, K.; Mortensen, N.A.; Xiao, S.; Ndoni, S.: 'Experimental demonstration of graphene plasmons working close to the near-infrared window', *Opt. Lett.* **2016**, 41 (22), pp. 5345-5348.
- [12] Xiao, B.; Sun, R.; He, J.; Qin, K.; Kong, S.; Chen, J.; Xiumin, W.: 'A Terahertz Modulator Based on Graphene Plasmonic Waveguide', *IEEE Photonics Technology Letters*, **2015**, 27, (20), pp. 2190-2192.
- [13] Vakil, A.; Engheta, N.: 'Transformation optics using graphene', *Science*, **2011**, 332, (6035), pp. 1291-1294.
- [14] Xiao, S.; Zhu, X.; Li, B.-H.; Mortensen, N. A.: 'Graphene-plasmon polaritons: From fundamental properties to potential applications', *Frontiers of Physics*, **2016**, 11, (2), pp. 1-13.
- [15] Ju, L.; Geng, B.; Horng, J.; Girit, C.; Martin, M.; Hao, Z.; Bechtel, H. A.; Liang, X.; Zettl, A.; Shen, Y. R.: 'Graphene plasmonics for tunable terahertz metamaterials', *Nature nanotechnology*, **2011**, 6, (10), pp. 630-634.
- [16] Yan, H.; Li, X.; Chandra, B.; Tulevski, G.; Wu, Y.; Freitag, M.; Zhu, W.; Avouris, P.; Xia, F.: 'Tunable infrared plasmonic devices using graphene/insulator stacks', *Nature nanotechnology*, **2012**, 7, (5), pp. 330-334.
- [17] Alaei, R.; Farhat, M.; Rockstuhl, C.; Lederer, F.: 'A perfect absorber made of a graphene micro-ribbon metamaterial', *Optics Express* **2012**, 20, (27), p. 28017.
- [18] Cheng, H.; Tian, J.; Li, J.; Deng, L.; Yu, P.; Chen, S.: 'Mid-infrared tunable optical polarization converter composed of asymmetric graphene nanocrosses', *Optics Letters* **2013**, 38, (9), pp. 1567-1569.
- [19] Fan, Y.; Shen, N.H.; Koschny, T.; Soukoulis, C.M.: 'Tunable Terahertz Meta-Surface with Graphene Cut-Wires', *Acs Photonics* **2015**, 2, (1), p. 150106103850009.
- [20] Zhu, Z.H.; Guo, C.C.; Liu, K.; Zhang, J.F.; Ye, W.M.; Yuan, X.D.; Qin, S.Q.: 'Electrically tunable polarizer based on anisotropic absorption of graphene ribbons', *Applied Physics A Materials Science & Processing* **2014**, 114, (4), pp. 1017-1021.
- [21] Xing, R.; Jian, S.: 'A dual-band THz absorber based on graphene sheet and ribbons', *Optics & Laser Technology*, **2018**, 100, pp. 129-132.
- [22] He, S.; Zhang, X.; He, Y.: 'Graphene nano-ribbon waveguides of record-small mode area and ultra-high effective refractive indices for future VLSI', *Optics Express* **2013**, 21, (25), p. 30664.
- [23] Su, Z.; Yin, J.; Zhao, X.: 'Terahertz dual-band metamaterial absorber based on graphene/MgF₂ multilayer structures', *Optics express*, **2015**, 23, (2), pp. 1679-1690.
- [24] Chen, M.; Sun, W.; Cai, J.; Chang, L.; Xiao, X.: 'Frequency-tunable terahertz absorbers based on graphene metasurface', *Optics Communications*, **2017**, 382, pp. 144-150.
- [25] Moreau, A.; Ciraci, C.; Mock, J. J.; Hill, R. T.; Wang, Q.; Wiley, B. J.; Chilkoti, A.; Smith, D. R.: 'Controlled-reflectance surfaces with film-coupled colloidal nanoantennas', *Nature*, **2012**, 492, (7427), pp. 86-89.
- [26] Chen, P. Y.; Alù, A.: 'Terahertz Metamaterial Devices Based on Graphene Nanostructures', *IEEE Transactions on Terahertz Science & Technology*, **2013**, 3, (6), pp. 748-756.
- [27] Hanson, G. W.: 'Dyadic Green's functions and guided surface waves for a surface conductivity model of graphene', *Journal of Applied Physics*, **2008**, 103, (6), p. 19912.
- [28] Nikitin, A. Y.; Guinea, F.; Garcia-Vidal, F. J.; Martin-Moreno, L.: 'Surface plasmon enhanced absorption and suppressed transmission in periodic arrays of graphene ribbons', *Physical Review B Condensed Matter*, **2011**, 85, (8), pp. 1123-1132.
- [29] Andryieuski, A.; Lavrinenko, A. V.: 'Graphene metamaterials based tunable terahertz absorber: effective surface conductivity approach', *Optics Express*, **2013**, 21, (7), pp. 9144-9155.
- [30] Wen, Q.-Y.; Zhang, H.-W.; Xie, Y.-S.; Yang, Q.-H.; Liu, Y.-L.: 'Dual band terahertz metamaterial absorber: Design, fabrication, and characterization', *Applied Physics Letters*, **2009**, 95, (24), p. 207402.
- [31] Zhang, C.; Cheng, H.; Pu, M.; Song, J.; Zhao, Z.; Wu, X.; Luo, X.: 'Dual-band wide-angle metamaterial perfect absorber based on the combination of localized surface plasmon resonance and Helmholtz resonance', *Scientific Reports* **2017**, 7, (1), p. 5652.

[32] Zhang, Y.; Li, T.; Chen, Q.; Zhang, H.; O'Hara, J.F.; Ethan, A.; Taylor, A.J.; Chen, H.T.; Azad, A.K.: 'Independently tunable dual-band perfect absorber based on graphene at mid-infrared frequencies', *Scientific Reports*, **2015**, 5, p. 18463.